Research article

Innate Immunity

16(6) (2010) 354–365
© SAGE Publications 2010
ISSN 1753-4259 (print)
10.1177/1753425909347400

The lipid A of *Burkholderia multivorans* C1576 smooth-type lipopolysaccharide and its pro-inflammatory activity in a cystic fibrosis airways model

Teresa Ieranò[1], Paola Cescutti[2], Maria Rosaria Leone[1], Alessandro Luciani[3], Roberto Rizzo[2], Valeria Raia[4], Rosa Lanzetta[1], Michelangelo Parrilli[1], Luigi Maiuri[5], Alba Silipo[1], Antonio Molinaro[1]

[1]*Dipartimento di Chimica Organica e Biochimica, Università degli Studi di Napoli Federico II, Napoli, Italy*
[2]*Dipartimento di Scienze della Vita, Università degli Studi di Trieste, Trieste, Italy*
[3]*Institute of Pediatrics, University of Foggia and Dynamic Imaging Microscopy, CEINGE, Naples, Italy*
[4]*Department of Pediatrics, Università degli Studi di Napoli Federico II, Naples, Italy*
[5]*Institute of Pediatrics, University of Foggia and European Institute for Research in Cystic Fibrosis San Raffaele Scientific Institute, Milan, Italy*

Cystic fibrosis is an autosomal recessive disorder and it is characterised by chronic bacterial airway infection which leads to progressive lung deterioration, sometimes with fatal outcome. *Burkholderia multivorans* and *Burkholderia cenocepacia* are the species responsible for most of the infections of cystic fibrosis patients. Lipopolysaccharide endotoxins (LPSs) are among the foremost factors of pathogenesis of Gram-negative infection and, in particular, lipid A is the endotoxic portion of LPS responsible for eliciting host innate immune response. In this work, the complete primary structure of the lipid A from *B. multivorans* C1576 has been defined and, further, its pro-inflammatory activity in a cystic fibrosis airways model is shown. The structure of *B. multivorans* lipid A was attained by chemical, mass spectrometry and nuclear magnetic resonance analyses whereas its biological activity was assessed on the intestinal epithelial cell line CACO-2 cells, on the airway epithelial IB3-1 cells, carrying the ΔF508/W1282X CFTR mutation and on an *ex vivo* model of culture explants of nasal polyps.

Keywords: Burkholderia multivorans, lipid A, lipopolysaccharide, mass spectrometry, cystic fibrosis

Introduction

Lipopolysaccharide endotoxins (LPSs) are the main molecules of the outer membrane of almost all Gram-negative bacteria and play a key role in the pathogenesis and in the toxic manifestation of Gram-negative infection.[1,2]

Structurally, they are amphiphilic macromolecules where a hydrophilic heteropolysaccharide is covalently linked to a lipophilic moiety termed lipid A[3–5] that anchors these macromolecules to the external membrane. Lipid A is the endotoxic portion of LPS responsible of the transmembrane signalling which stimulates the mammalian innate immune response. Actually, it has been demonstrated that, in mammals, Toll-like receptor 4 (TLR4) serves as the main upstream sensor for LPS effects *in vitro* and *in vivo*.[6–8] Toll-like receptor 4 is part of a trimolecular LPS receptor complex[8] that contains two co-receptors: (i) MD2, a secreted accessory protein required for the correct positioning of TLR4 on the cell surface and for TLR4 transmembrane signal transduction;[8] and (ii) CD14,

Received 23 April 2009; Revised 5 August 2009; Accepted 7 August 2009

Correspondence to: Antonio Molinaro, Dipartimento di Chimica Organica e Biochimica, Università degli Studi di Napoli Federico II, Via Cintia 4, I-80126 Napoli, Italy. Tel: +39 (0)81 674123; Fax: +39 (0)81 674393; E-mail: molinaro@unina.it

which exists in soluble form (s-CD14) or as a high-affinity glycosyl-phosphatidyl inositol-linked-LPS-binding protein (m-CD14).[6] Thus, lipid A is the LPS moiety that is crucial in eliciting mammalian innate immunity, it represents the pathogen-associated molecular pattern (PAMP) involved in such recognition process, *i.e*. it is recognized as the endotoxic principle. After lipid A detection by the TLR4–MD2 receptor complex, the host initiates a rapid and massive immune response that includes the generation of a complex cascade of cellular mediators among which tumor necrosis factor-α (TNF-α) appears to be important for the development of endotoxic shock.[7] Actually, if the low and balanced concentrations of these immune-response mediators allows the host to respond to the invading pathogen, the spread of the infection and the successive pathophysiological over-reaction leads to the release of toxic amounts of these cellular mediators. Lipid A endotoxic and pro-inflammatory activity varies strongly with its primary structure, namely, fatty acids, polar heads and carbohydrate components.[9]

Beside *Pseudomonas aeruginosa*, *Burkholderia multivorans* and *Burkholderia cenocepacia* are the species responsible of most of the infections of cystic fibrosis patients. Cystic fibrosis is the most common autosomal recessive disorder in Europe and North America (1 in 2500 live births) and it is characterised by chronic bacterial airway infection which leads to progressive lung deterioration, sometimes with fatal outcome. Although *B. cenocepacia* is the predominant species in most cystic fibrosis centers, the situation is different in the UK, where in latterly the isolation of *B. multivorans* exceeded that of *B. cenocepacia*.[10] In particular, the isolate used in this study, *B. multivorans* C1576, is one of the Edinburgh collection representing the Glasgow outbreak[11] when few cystic fibrosis children survived to adulthood; this isolate was also included in the panel of reference strains from the *B. cepacia* complex.[12] In this work, we define the complete primary structure of the lipid A obtained from *B. multivorans* C1576 and, further, we show its pro-inflammatory activity in a cystic fibrosis airways model. Such data are an essential prerequisite to elucidate the inflammatory process following infection. Understanding how bacteria behave in the infection may allow greater understanding of LPS-associated signalling.

The structure of *B. multivorans* lipid A was attained by chemical, mass spectrometry (MS) and nuclear magnetic resonance (NMR) analyses whereas its biological activity was assessed on the intestinal epithelial cell line CACO-2 cells, on the IB3-1 cells, carrying the ΔF508/W1282X CFTR mutation and on an *ex vivo* model of culture explants of nasal polyps.

Materials and Methods

Bacterial growth and LPS extraction

Burkholderia. multivorans strain C1576 was a kind gift of Prof. J.R.W. Govan (Centre for Infectious Diseases, University of Edinburgh Medical School, Edinburgh, UK). The bacteria were cultured in liquid Luria Bertani medium enriched with 0.2% glucose for 3 at 30°C with shaking. The broth culture was centrifuged, the cells were washed with 0.5% NaCl and freeze-dried (yield 16 g of dried cells).

LPS was extracted by the hot phenol/water procedure as described[13] and revealed by sodium dodecyl sulfate polyacrylamide gel electrophoresis (SDS-PAGE, 12%). The gel was stained with silver nitrate for detection of LPSs. In order to remove all the cell contaminants, the LPS fraction was further subjected to enzymatic hydrolysis with RNAse, DNAse and proteinase K followed by a size-exclusion chromatography on Sephacryl S-300 in 50 mM NH_4CO_3 (yield 170 mg, 1.5% of dried cells).

Preparation of lipid A and O*-deacylated lipid A*

Free lipid A was obtained by treatment of LPS (30 mg) with 0.1 M sodium acetate buffer (pH 4.4) containing 1% SDS (100°C, 3 h). The solution was then lyophilized, treated with 2 M HCl-EtOH (1:100, v:v) to remove the SDS, evaporated, dissolved in water and ultracentrifuged (100,000 *g*, 4°C, 90 min). The obtained precipitate (free lipid A) was washed with water (yield: 4.8 mg, 16% of the LOS). Thin-layer chromatography (TLC) of lipid A was carried out on Silica Gel 60 TLC plates (20 × 20 cm, 0.25 μm thickness), eluted with $CHCl_3$/MeOH/H_2O (100:75:15, by vol.) and $CHCl_3$/MeOH/H_2O/triethylamine (30:12:2:0.1).[14] Compounds were visualized by spraying the plate with 10% ethanolic H_2SO_4 and charring. Lipid A was partially *O*-deacylated by treatment with 12% NH_4OH at 25°C for 18 h,[15] whereas it was completely *O*-deacylated by anhydrous hydrazine.

General and analytical procedures

Monosaccharides were identified as acetylated *O*-methylglycoside derivatives. After methanolysis (2 M HCl-MeOH, 85°C, 24 h) and acetylation with acetic anhydride in pyridine (85°C, 30 min) the sample was analyzed by GC-MS. Monosaccharides were derivatized as acetylated *O*-oct-2-yl-glycosides in order to obtain their absolute configuration according to the published method.[16] Methylation analysis was carried out on dephosphorylated product obtained by keeping it at 4°C, 48 h, in HF 48% (200 μl) and then evaporated under a stream of nitrogen. Methylation was performed

with methyl iodide in sodium hydroxide as described.[17] The hydrolysis of the methylated sugar backbone was performed with 4 M trifluoroacetic acid (100°C, 4 h) and the partially methylated product, after reduction with $NaBH_4$, was converted into alditol acetates with acetic anhydride in pyridine at 80°C for 30 min and analyzed by GLC-MS as described below. Total fatty acid content was obtained by acid hydrolysis of lipid A. Briefly, lipid A was first treated with 4 M HCl (4 h, 100°C) and then with 5 M NaOH (30 min, 100°C). The solution was then acidified and fatty acids were extracted in $CHCl_3$, methylated with diazomethane and analyzed by GLC-MS. The ester bound fatty acids were selectively released by base-catalyzed hydrolysis with 0.5 M NaOH-MeOH (1:1 v/v, 85°C, 2 h), then the product was acidified, extracted in $CHCl_3$, methylated with diazomethane and analyzed by GLC-MS. The absolute configuration of fatty acids was determined by chemical derivatization and GLC-MS.[14] All GLC analyses were performed on a Hewlett-Packard 5890 instrument, SPB-5 capillary column (0.25 mm × 30 m, Supelco); for sugar methylation analysis and *O*-methyl glycosides derivatives the temperature program was 150°C for 2 min, then 2°C/min to 200°C for 0 min, then 10°C/min to 260°C for 11 min, then 8°C/min to 300°C for 20 min; for absolute configuration analysis it was 150°C for 8 min, then 2°C/min to 200°C for 0 min, then 6°C/min to 260°C for 5 min. For fatty acid analysis, the temperature program was 80°C for 2 min, then 8°C/min to 300°C for 15 min. Nuclear magnetic resonance experiments were carried out as described.[14]

Mass spectrometry

Electrospray source ionisation (ESI) mass spectra were recorded on a Bruker Esquire 4000 ion trap mass spectrometer connected to a syringe pump for the injection of the samples. The instrument was calibrated using a tune mix given by Bruker. Before MS analysis, a small amount of lipid A was resuspended in 400 µl of water, stirred on a vortex and centrifuged. The pellet was treated again in the same manner, freeze-dried and used for MS analysis. Samples were dissolved in a chloroform:methanol (2:1 mixture) in a suitable concentration, injected at 180 µl/h, and detected in the negative ion mode. When the spectra were recorded in the positive ion mode, 3 µl of a 0.75 M ammonium acetate solution were added to 200 µl of sample dissolved in chloroform:methanol (2:1, v/v).

Patients and ex vivo *cultures of nasal polyp mucosal biopsies*

Five consecutive cystic fibrosis patients carrying the common CFTR mutations (F508del/F508del, F508del/W1282X) with idiopathic polyposis underwent surgical treatment. Informed consent was obtained from all subjects and the ethical committee of Regione Campania Health Authority approved the study.

Nasal polyp explants were cultured, as previously reported[18] for 4–24 h with 1 µg/ml LPS from *P. aeruginosa*, or 1 µg/ml of *B. multivorans* lipid A (BMLA) in the presence or absence of the selective p38 MAP kinase inhibitor SB253080. SB203580 was used at a concentration of 1 µM considered to be specific for the p38-MAP-kinase, although effects on other signal transduction pathways might still occur.

Cell culture

Human cystic fibrosis bronchial epithelial cell line IB3-1, carrying the F508del/W1282X CFTR mutation, or intestinal CACO-2 cell line (LGC Promochem, Milan, Italy) were cultured as recommended by the American Type Culture Collection (ATCC).

CACO-2 cell lines were incubated with 1 µg/ml LPS from *Escherichia coli*, or 1 µg/ml lipid A from *B. multivorans*. IB3-1 cell lines were incubated with 0.5, 2, 2, 5, 10, 100 µg/ml LPS from *P. aeruginosa* or lipid A from *B. multivorans*.

Confocal microscopy: human tissue sections

The detection of antigen expression and distribution on tissue specimens was performed by incubating the sections with antibodies against Py99 (clone sc72020, Santa Cruz Biotechnology) or COX-2 (Cell Signaling) as previously described.[18]

Cell lines

Treated or untreated cells were fixed in methanol, permeabilized with 0.5% Triton X-100 and incubated with antibodies against Py99 (clone 72020, Santa Cruz Biotechnology) according to the previously described procedure.[19]

ELISA tests

Human TNF-α or IL-8 secretion was measured using the Cytometric Bead Array (BD Biosciences, NJ, USA) using a FACScan (BD Biosciences). Measurements were performed at least in triplicate. Values were normalized to 10^6 cells; results were expressed as mean ± SEM.

Statistical analysis

All experiments were performed at least in triplicate. Data distribution was analyzed, and statistical differences were evaluated by using ANOVA Tukey–Kramer test by SPSS v.12 software. A P-value of <0.05 was considered significant.

RESULTS

Extraction of LPS and compositional analysis of intact lipid A

Sodium dodecyl sulfate-PAGE of the LPS fraction obtained by extraction of dried cells showed the typical run of a smooth type LPS with a ladder-like pattern. The LPS was further purified from other cell contaminants by enzymatic hydrolysis with DNAse, RNAse and proteinase K followed by dialysis and a gel-permeation chromatography. Lipid A was obtained by SDS promoted mild acid hydrolysis. Compositional analysis of the obtained methyl and chiral butyl glycosides[16] revealed the presence of GlcN with D-configuration, and of 4-amino-4-deoxy-arabinose (Ara4N) with L-configuration whereas methylation analysis showed the presence of 6-substituted-GlcN, terminal-GlcN and terminal Ara4N.

Fatty acid analysis revealed the presence of (*R*)-3-hydroxyhexadecanoic [16:0(3-OH)] in amide-linkage and of (*R*)-3-hydroxytetradecanoic [14:0(3OH)] and tetradecanoic acid (14:0) in ester-linkage.

ESI MS of intact lipid A

The ESI mass spectrum of lipid A recorded in the negative ion mode showed a complex pattern of [M-H]- molecular ions (Table 1 and Fig. 1A), characterised by seven main species (**3**, **4**, **5**, **6**, **9**, **12**, and **15** in Table 1) and other minor peaks, representing an array of tri- to penta-acylated species.[20,21] The most intense pseudomolecular ion at *m/z* 1495.2 (species **4**) was assigned to a monophosphorylated glucosamine disaccharide backbone substituted by one 14:0(3-OH), one 14:0, two 16:0(3-OH) and one Ara4N residue, while the ion at *m/z* 1364.1 (species **3**) corresponded to the previous one lacking the Ara4N residue. Interestingly, a tetra-acylated lipid IVa analogue[2–5] (species **5**) was also present at *m/z* 1511.2; specifically, a mono-phosphorylated lipid A ion carrying all primary fatty acids (two 16:0(3-OH), two 14:0(3-OH)) and additionally bearing a phosphoryl Ara4N group. The ion at *m/z* 1590.3 (species **6**) was attributed to a penta-acylated (two 16:0(3-OH), two 14:0(3-OH) and one 14:0) monophosphorylated glucosamine disaccharide backbone, while species **9** at *m/z* 1721.3 carried an additional Ara4N residue. The ion at *m/z* 1823.3 (species **12**) was attributed to a *bis*-phosphorylated penta-acylated species with one Ara4N residue whereas species **15** contained an additional Ara4N residue.

Table 1. ESI MS negative pseudomolecular ions of lipid A from *B. multivorans*

Observed ion [*m/z*]	Species	Acyl substitution	Proposed fatty acid, phosphate and carbohydrate composition
1269.0	**1**	Tri-acyl	2 × 16:0(3-OH), 1 × 14:0, 1 × Ara4N, 1 P
1284.9	**2**	Tri-acyl	2 × 16:0(3-OH), 1 × 14:0(3-OH), 1 × Ara4N, 1 P
*1364.1	**3**	Tetra-acyl	2 × 16:0(3-OH), 1 × 14:0(3-OH), 1 × 14:0, 1 P
*1495.2	**4**	Tetra-acyl	2 × 16:0(3-OH), 1 × 14:0(3-OH), 1 × 14:0, 1 × Ara4N, 1 P
*1511.2	**5**	Tetra-acyl	2 × 16:0(3-OH), 2 × 14:0(3-OH), 1 × Ara4N, 1P
*1590.3	**6**	Penta-acyl	2 × 16:0(3-OH), 2 × 14:0(3-OH), 1 × 14:0, 1 P
1597.1	**7**	Tetra-acyl	2 × 16:0(3-OH), 1 × 14:0(3-OH), 1 × 14:0, 1 × Ara4N, 2 P, 1 Na^+
1606.2	**8**	Penta-acyl	2 × 16:0(3-OH), 3 × 14:0(3-OH), 1 P
*1721.3	**9**	Penta-acyl	2 × 16:0(3-OH), 2 × 14:0(3-OH), 1 × 14:0, 1 × Ara4N, 1 P
1728.2	**10**	Tetra-acyl	2 × 16:0(3-OH), 1 × 14:0(3-OH), 1 × 14:0, 2 × Ara4N, 2 P, 1 Na^+
1737.3	**11**	Penta-acyl	2 × 16:0(3-OH), 3 × 14:0(3-OH), 1 × Ara4N, 1 P
*1823.3	**12**	Penta-acyl	2 × 16:0(3-OH), 2 × 14:0(3-OH), 1 × 14:0, 1 × Ara4N, 2 P, 1 Na^+
1839.2	**13**	Penta-acyl	2 × 16:0(3-OH), 3 × 14:0(3-OH), 1 × Ara4N, 2 P, 1 Na^+
1851.3	**14**	Penta-acyl	3 × 16:0(3-OH), 1 × 14:0(3-OH), 1 × 14:0, 1 × Ara4N, 2 P, 1 Na^+
*1954.3	**15**	Penta-acyl	2 × 16:0(3-OH), 2 × 14:0(3-OH), 1 × 14:0, 2 × Ara4N, 2 P, 1 Na^+
1970.4	**16**	Penta-acyl	2 × 16:0(3-OH), 3 × 14:0(3-OH), 2 × Ara4N, 2 P, 1 Na^+
1982.3	**17**	Penta-acyl	3 × 16:0(3-OH), 1 × 14:0(3-OH), 1 × 14:0, 2 × Ara4N, 2 P, 1 Na^+

Main peaks are marked with an asterisk and also shown in Figure 1A. Observed ions correspond to [M-H]-monoisotopic ions.

The assignment of all the other ions, characterised by a much lower intensity, will not be discussed in detail but it is reported in Table 1. An expansion of the ESI mass spectrum showing some of these less intense ions is also reported in the inset of Figure 1A. They are characterised by variations in the number of acyl substituents, Ara4N residues, phosphate groups and Na^+ present as counter ions of the phosphate groups.

ESI MS-MS of intact lipid A

In order to assign the primary structure and location of the substituents of the lipid A polymorphic fraction fully, MS-MS experiments were carried out.

Isolation and fragmentation in the negative ion mode of the pseudomolecular ion at *m/z* 1495.1 gave rise to fragments formed by loss of 14:0(3-OH) and Ara4N (Fig. 1B), the former suggesting substitution at 3 and /or 3' position of the glucosamine residues with 14:0(3-OH) fatty acid chains.

The positive ion-mode ESI mass spectrum showed just two main monophosphorylated sodium adducts at *m/z* 1162.0 and 1388.0: the first was ascribed to a tri-acylated species (two 16:0(3-OH) and one 14:0 chains) while the second was attributed to a tetra-acylated species (two 16:0(3-OH), one 14:0(3-OH) and one 14:0 chains; spectrum not shown). A signal with low intensity at *m/z* 1541.0 was attributed to the above described tetra-acylated species, substituted with a

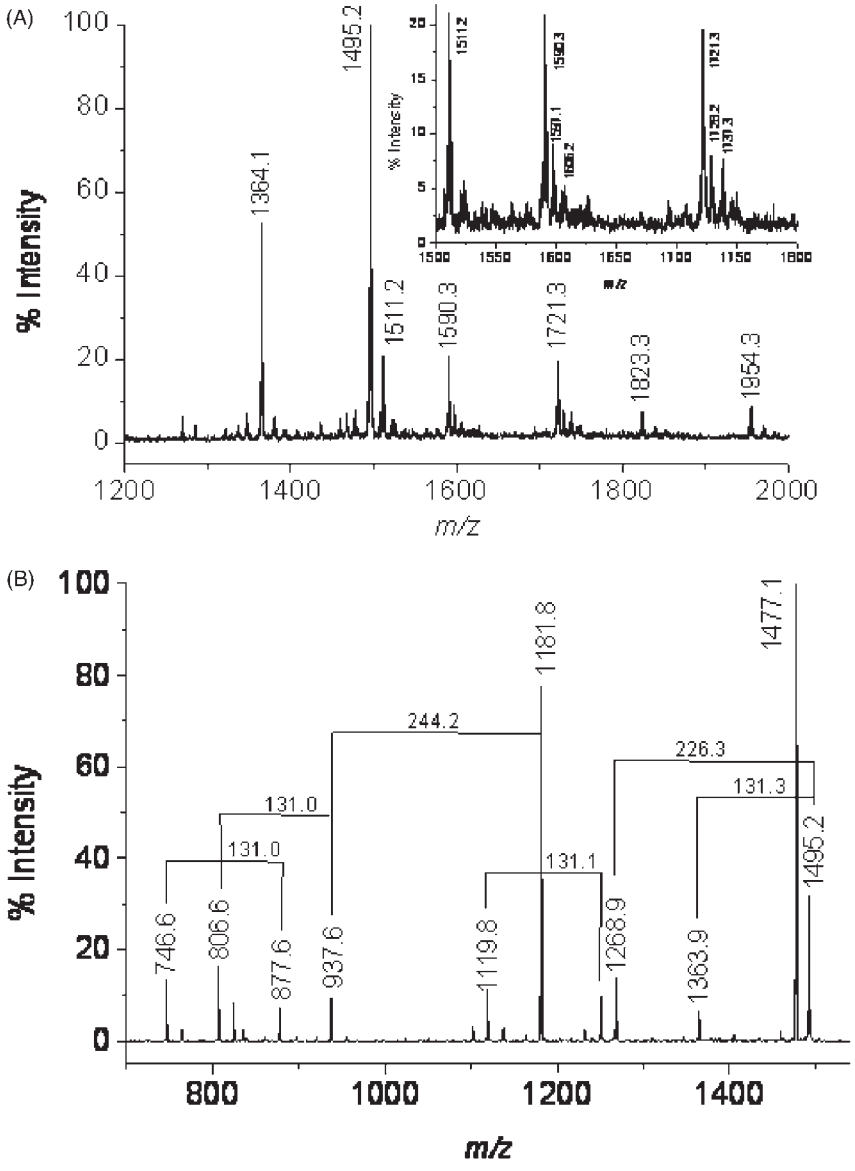


Fig. 1. ESI mass spectrum recorded in the negative ion mode of a lipid A sample (A). In the inset, an enlargement of the spectrum with less intense signals is shown. MS^2 of the ion at *m/z* 1495.1 in the negative ion mode (B).

Ara4N residue and carrying a sodium counter ion (data not shown). Isolation and fragmentation of the ion at *m/z* 1388.0 resulted in the identification of the oxonium ion at *m/z* 954.7 (Fig. 2A) to which was assigned the following composition: one GlcN, one phosphate group with sodium as counter ion, one 16:0(3-OH), one 14:0(3-OH) and one 14:0 chain. A high intensity signal at *m/z* 726.5 consistent with loss of the 14:0 fatty acid (228 Da) suggested that it was linked to the acyl amide moiety, as previously reported.[22] Thus, it was also possible to ascertain that in the monophosphorylated species the phosphate group is located on the O-4 of non

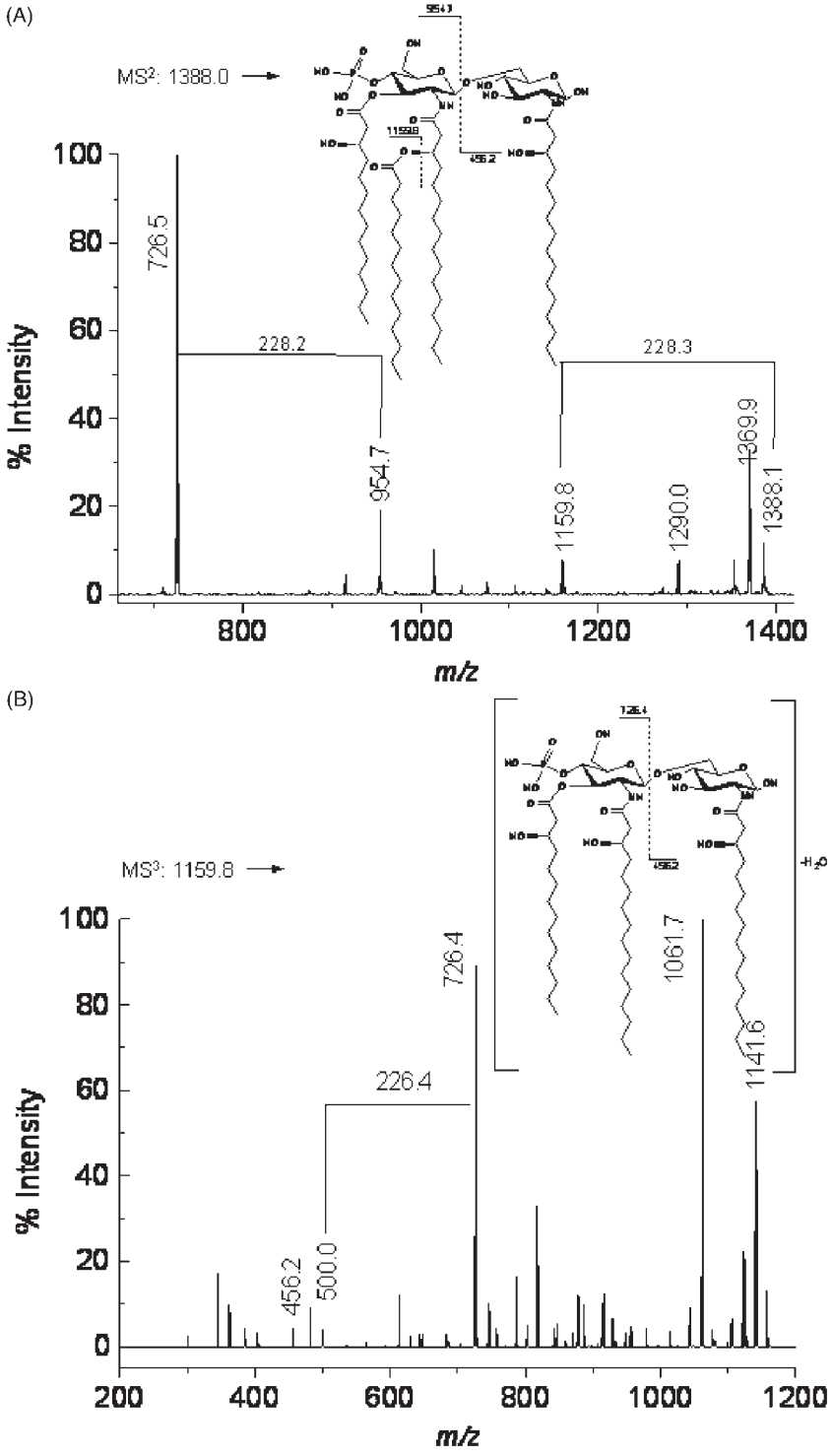


Fig. 2. MS^2 fragmentation spectrum of the ion at *m/z* 1388.0 (A) and MS^3 fragmentation spectrum of the ion at *m/z* 1159.8 (B) both obtained in the positive ion mode.

reducing GlcN II. In the same spectrum, the ion at *m/z* 1159.8 was due to loss of a 14:0 fatty acid together with water. Its MS^3 mass spectrum (Fig. 2B) was very informative, since it showed ions deriving from the reducing as well as non-reducing ends. The species at *m/z* 726.4 was consistent with an oxonium ion with the following composition: one GlcN, one phosphate group with sodium as counter ion, one 16:0(3-OH), and one 14:0(3-OH). In the same spectrum, the signal at *m/z* 456.2 was assigned to the sodium adduct of the reducing end GlcN residue acylated with 16:0(3-OH). Isolation and fragmentation of the ion at *m/z* 1541.0 to establish the position of L-Ara4N was unsuccessful, because of the low intensity of this signal, and no oxonium ions were observed. However, the oxonium ions at *m/z* 954.7 and 726.4 clearly showed that the phosphate group is located on the GlcN at the non-reducing end, therefore signifying that the Ara4N substituent is also present on the same GlcN residue, given that it is always linked via phosphate.

ESI MS of O*-deacylated lipid A*

An aliquot of lipid A was selectively *O*-deacylated by treatment with NH_4OH and then subjected to ESI MS analysis. In this way, the amide-bound acyloxyacyl moieties were identified, since they were left unaltered by this selective ester hydrolysis reaction.[15] The negative ion mode ESI mass spectrum obtained is reported in Figure 3. As for the native lipid A, the mass spectrum showed some intense signals (species **18**, **19**, **22**, **24**, **27**, and **31** in Table 2) accompanied with other less intense ion peaks. The majority of the molecular forms obtained after NH_4OH treatment derived from loss of one 14:0(3-OH) chain ($\Delta = 226.19$ amu) from species present in the native sample. A smaller number of ions (species **18**, **20** and **21**) derived from loss of one 14:0 chain from molecular species present in the native sample. The pseudomolecular ion at *m/z* 1058.8 (species **18**) was attributed to a di-acylated monophosphorylated lipid A bearing a Ara4N residue and two 16:0(3-OH) chains in amide linkage. The two main ions at *m/z* 1137.9, and 1268.9 (species **19** and **22**) corresponded to tri-acylated (two 16:0(3-OH), one 14:0), monophosphorylated molecules differing for the presence of L-Ara4N ($\Delta m/z = 131.06$). The third intense ion at *m/z* 1364.0 (species **24**) was assigned to a tetra-acylated form deriving from the loss of one 14:0(3-OH) chain from species **6**. The ions at *m/z* 1597.0 and 1728.0 (species **31** and **32**) corresponded to a tetra-acylated, *bis*-phosphorylated forms differing for the content in Ara4N residues (Table 2). The assignment of the less intense ions is not discussed in detail but it is reported in Table 2.

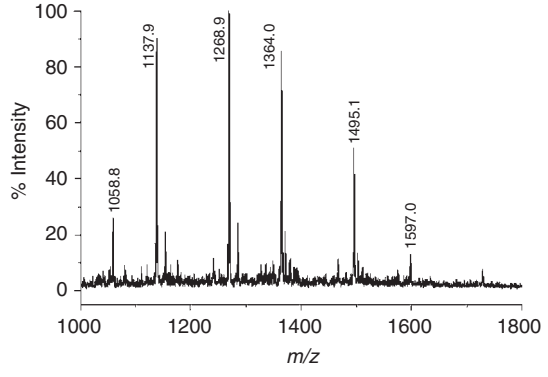


Fig. 3. ESI mass spectrum recorded in the negative ion mode of a sample of lipid A after *O*-deacylation with NH_4OH.

In agreement with what was already found in the intact sample, the positive ion mode ESI mass spectrum revealed two main sodium adducts at *m/z* 1161.8 and 1388.0. Isolation and fragmentation of the ion at *m/z* 1161.8 (data not shown) yielded an oxonium ion at *m/z* 728.5 composed by one GlcN, one sodium phosphate group, one 16:0 (3-OH) and one 14:0 chain. The loss of 228 Da (the 14:0 fatty acid) from the ion at *m/z* 728.5 resulted in a high intensity ion at *m/z* 500.3, confirming the location of the 14:0 chain on the 16:0 (3-OH) sitting on the non-reducing GlcN residue, in agreement with the data found for the native lipid A.

NMR spectroscopy of lipid A

A combination of homo- and hetero-nuclear NMR experiments were performed in $CHCl_3$:MeOH:H_2O (2:3:1, v/v) on the *O*-deacylated lipid A aiming at defining the carbohydrate backbone. Double quantum filtered-correlation spectroscopy (COSY), total correlation spectroscopy (TOCSY), rotating frame Overhauser enhancement spectroscopy (ROESY), ^{13}C-^{1}H and ^{31}P-^{1}H heteronuclear single quantum coherence (HSQC) spectra were used to assign ^{13}C, ^{1}H and ^{31}P resonances. The NMR data revealed the presence of the typical β-D-GlcPN-(1→6)-α-D-GlcPN disaccharide backbone with a variety of acyl chains that resulted in a heterogeneous mixture of species all sharing the *N*-acylation. The presence in non-stoichiometric amount of a β-L-Arap4N residue attached via phosphodiester bond at O-4 of GlcN II was demonstrated ^{31}P-^{1}H HSQC where a correlation between H-4 of GlcN II and the anomeric proton of Ara4N was evident. Conversely, the anomeric position of GlcN I was either present as free reducing end or, when bound to phosphate, as α-configured residue. All the other chemical shifts and correlations in the NMR spectra were similar to those obtained for *B. cepacia* and *B. caryophylli* lipid A, thus they are not discussed further.[14,23] In conclusion, all data on the selectively degraded lipid A converged to a heterogeneous mixture

Table 2. ESI MS negative pseudomolecular ions of lipid A from *B. multivorans* after NH_4OH treatment

Observed ion [*m/z*]	Species	Acyl substitution	Proposed fatty acid, phosphate and carbohydrate composition
*1058.8	**18**	Di-acyl	2 × 16:0(3-OH), 1 × Ara4N, 1 P
*1137.9	**19**	Tri-acyl	2 × 16:0(3-OH), 1 × 14:0, 1 P
1153.9	**20**	Tri-acyl	2 × 16:0(3-OH), 1 × 14:0(3-OH), 1 P
1175.9	**21**	Tri-acyl	2 × 16:0(3-OH), 1 × 14:0(3-OH), 1 P, 1 Na^+
*1268.9	**22**	Tri-acyl	2 × 16:0(3-OH), 1 × 14:0, 1 × Ara4N, 1 P
1284.9	**23**	Tri-acyl	2 × 16:0(3-OH), 1 × 14:0(3-OH), 1 × Ara4N, 1 P
*1364.0	**24**	Tetra-acyl	2 × 16:0(3-OH), 1 × 14:0(3-OH), 1 × 14:0, 1 P
1370.9	**25**	Tri-acyl	2 × 16:0(3-OH), 1 × 14:0, 1 × Ara4N, 2 P, 1 Na^+
1380.1	**26**	Tetra-acyl	2 × 16:0(3-OH), 2 × 14:0(3-OH), 1 P
*1495.1	**27**	Tetra-acyl	2 × 16:0(3-OH), 1 × 14:0(3-OH), 1 × 14:0, 1 × Ara4N, 1 P
1501.9	**28**	Tri-acyl	2 × 16:0(3-OH), 1 × 14:0, 2 × Ara4N, 2 P, 1 Na^+
1511.1	**29**	Tetra-acyl	2 × 16:0(3-OH), 2 × 14:0(3-OH), 1 × Ara4N, 1 P
1575.0	**30**	Penta-acyl	2 × 16:0(3-OH), 1 × 14:0(3-OH), 1 × 14:0, 1 × Ara4N, 2 P
*1597.0	**31**	Penta-acyl	2 × 16:0(3-OH), 1 × 14:0(3-OH), 1 × 14:0, 1 × Ara4N, 2 P, 1 Na^+
1728.0	**32**	Tetra-acyl	2 × 16:0(3-OH), 1 × 14:0(3-OH), 1 × 14:0, 2 × Ara4N, 2 P, 1 Na^+

Main peaks are marked with an asterisk and also shown in Figure 3. Observed ions correspond to [M-H]-monoisotopic ions.

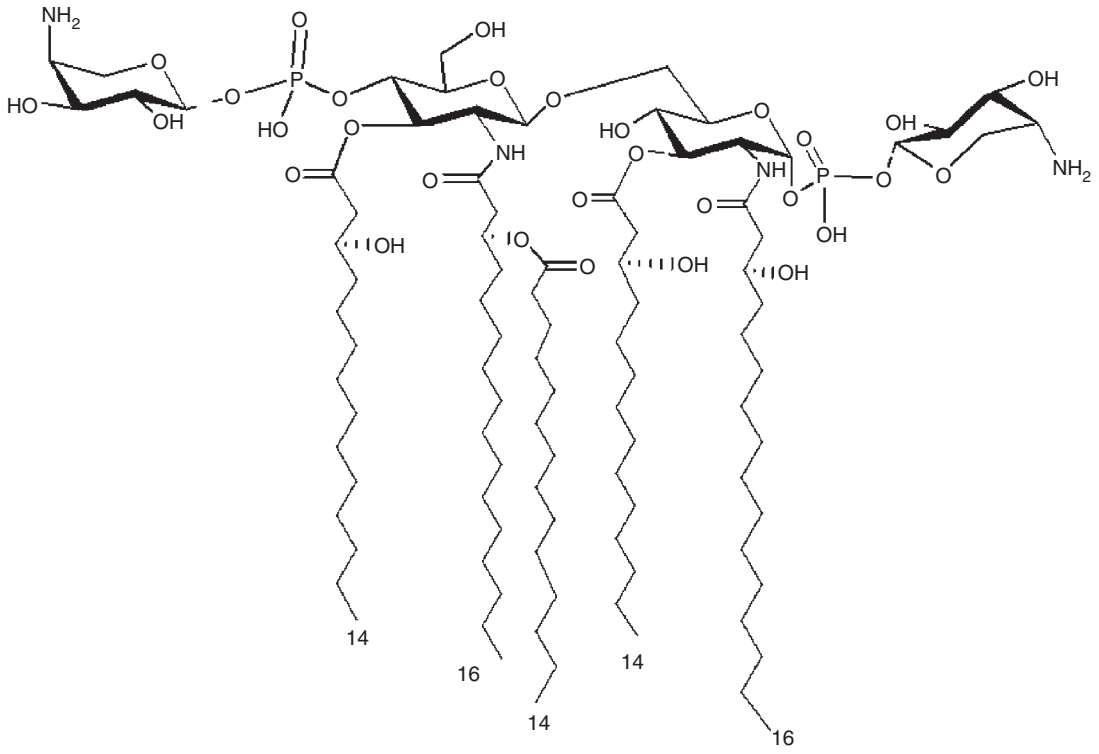


Fig. 4. The full structure of the lipid A from *B. multivorans* C1576 smooth-type lipopolysaccharide. Dotted lines indicate the non-stoichiometric substitutions (see text, figures and Table 1).

of tetra- and penta-acylated species differing by phosphorylation pattern and substitution by Ara4N (Fig. 4).

All information gained from the experiments described above together with the data reported in Figure 1 and Table 1 led to a complete picture of lipid A primary structure from *B. multivorans* C1576. The highest mass ion peak, **15** at *m/z* 1954.3 [M+Na^+] is consistent with a penta-acylated disaccharide backbone substituted by two phosphoryl-arabinosamine residues β-L-AraP4N-1-P → 4-β-L-GlcPN-(1→6)-α-L-GlcPN-1 → P-1-β-L-AraP4N, carrying in ester linkage two 14:0(3-OH) chains and in amide linkage, two

16:0(3-OH) chains, one of which, on the GlcN II, is further substituted by a secondary fatty acid, a 14:0 residue. Species **12** (*m/z* 1823.3) lacks one Ara4N residue, while species **9** (*m/z* 1721.3) lacks also a phosphate group and bears one Ara4N on non-reducing GlcN II. The ion **6** consists of a monophosphorylated penta-acylated lipid A bearing only one phosphate with no other sugar units than the disaccharide backbone. The two major ion species (**3** and **4**) of the mass spectrum both consisted in tetra-acylated mono-phosphorylated species. The ion at *m/z* 1364.1 lacked the anomeric phosphate and a primary *O*-linked 14:0(3-OH) on one of the GlcN residues whereas, as only difference, the ion peak at *m/z* 1495.2 possessed a further Ara4N residue linked to GlcN II via phosphodiester bond. On the same basis, species **5** could be defined as a unique tetra-acylated species bearing all primary fatty acids and phosphoryl-arabinosamine group at GlcN II whereas it possessed a free reducing end.

Effects of B. multivorans *lipid A on intestinal CACO-2 cell line*

To assess whether *B. multivorans* lipid A is endowed with biological activity, we investigated whether it was effective in inducing epithelial activation in different cell culture models. First, the biological activity was analysed in a widely used intestinal epithelial cell line. CACO-2 cells were cultured for 24 h in the presence of *E. coli* LPS or lipid A from *B. multivorans*. LPS from *E. coli* was used as a well-known inducer of epithelial activation.[18,19] The effects on tyrosine phosphorylation, a marker of epithelial activation,[19] were assessed by confocal microscopy using the Py-99 antibody. Confocal images revealed that lipid A from *B. multivorans* was as effective as *E. coli* LPS in enhancing membrane tyrosine phosphorylation (Fig. 5A).

Effects of B. multivorans *lipid A on cystic fibrosis airways*

To investigate whether *B. multivorans* lipid A was effective in triggering an inflammatory response in cystic fibrosis airways, we used an epithelial cell line carrying a common ΔF508/W1282X CFTR mutation. These cystic fibrosis airway epithelial cells show a constitutive inflammatory phenotype as a consequence of defective CFTR function,[18] and are hyper-responsive to LPS stimulation. In our experiments, lipid A stimulation in IB3 cells increased TNF-α expression (Fig. 5B), as compared to unstimulated cells. In a further series of experiments, we tested the effects of different concentrations (0.5–100 μg/ml) of lipid A as compared to *P. aeruginosa* LPS and found overlapping results (Fig. 5C). This indicates that it is as effective as *P. aeruginosa* LPS stimulation.[1]

In order to assess whether lipid A was relevant in triggering inflammation *in vivo* in cystic fibrosis airways, an *ex vivo* model of culture explants of nasal polyps was used.[18] In such a model, it was tested whether *B. multivorans* lipid A was as effective as *P. aeruginosa* LPS that was already reported to induce dramatic epithelial activation upon 4 h challenge of cystic fibrosis biopsies.[18] Even in this case, *B. multivorans* lipid A was highly effective in inducing tyrosine phosphorylation (Fig. 5D) and COX-2 expression with respect to the pattern observed in unstimulated nasal polyp mucosae (Fig. 5E). Moreover, the increase of IL-8 protein levels was detected in culture supernatants upon lipid A stimulation (Fig. 5F). These effects were similar to those obtained upon *P. aeruginosa* LPS stimulation. Moreover lipid A induced p38-MAP-kinase (p38-MAPK) phosphorylation (data not shown), a key player in the inflammatory cascade triggered by *P. aeruginosa* LPS in cystic fibrosis airways.[18] The role of p38-MAPK pathway was confirmed by using the specific p38-MAPK inhibitor SB203580 that was effective in controlling lipid A mediated tyrosine phosphorylation (Fig. 5G) and COX-2 protein expression (Fig. 5H). The same effects were observed after incubation with *B. multivorans* lipid A LPS (Fig. 5D and data not shown)

DISCUSSION

Gram-negative LPS lipid A contributes to the majority of endotoxic activity of LPS and subsequently to the elicitation of host innate immunity. Besides the effects of the other and most variable LPS portions in triggering the responses of the host-acquired immune system, the biological activity of the different strains within the genus depends on the phosphorylation, glycosylation and acylation pattern of lipid A backbone. The activation of the innate immune system is, in fact, performed by the natural blend of different lipid A species produced by the bacterium; pathogenic strains likely express higher percentages of lipid A agonists and this may be one of the reasons of the elevated response observed in the colonized organisms.

We have previously described the LOS from *B. multivorans* from a cystic fibrosis patient subjected to lung transplantation, which, in that case, was the sole component of the LPS fraction.[24] It was built up of a core oligosaccharide and a lipid A that possessed a comparable amount of penta- and tetra-acylated species with a notable abundance of Ara4N moieties; in contrast, in *B. multivorans* C1576 smooth-type LPS, the polysaccharide part is attached to a lipid A that possesses a

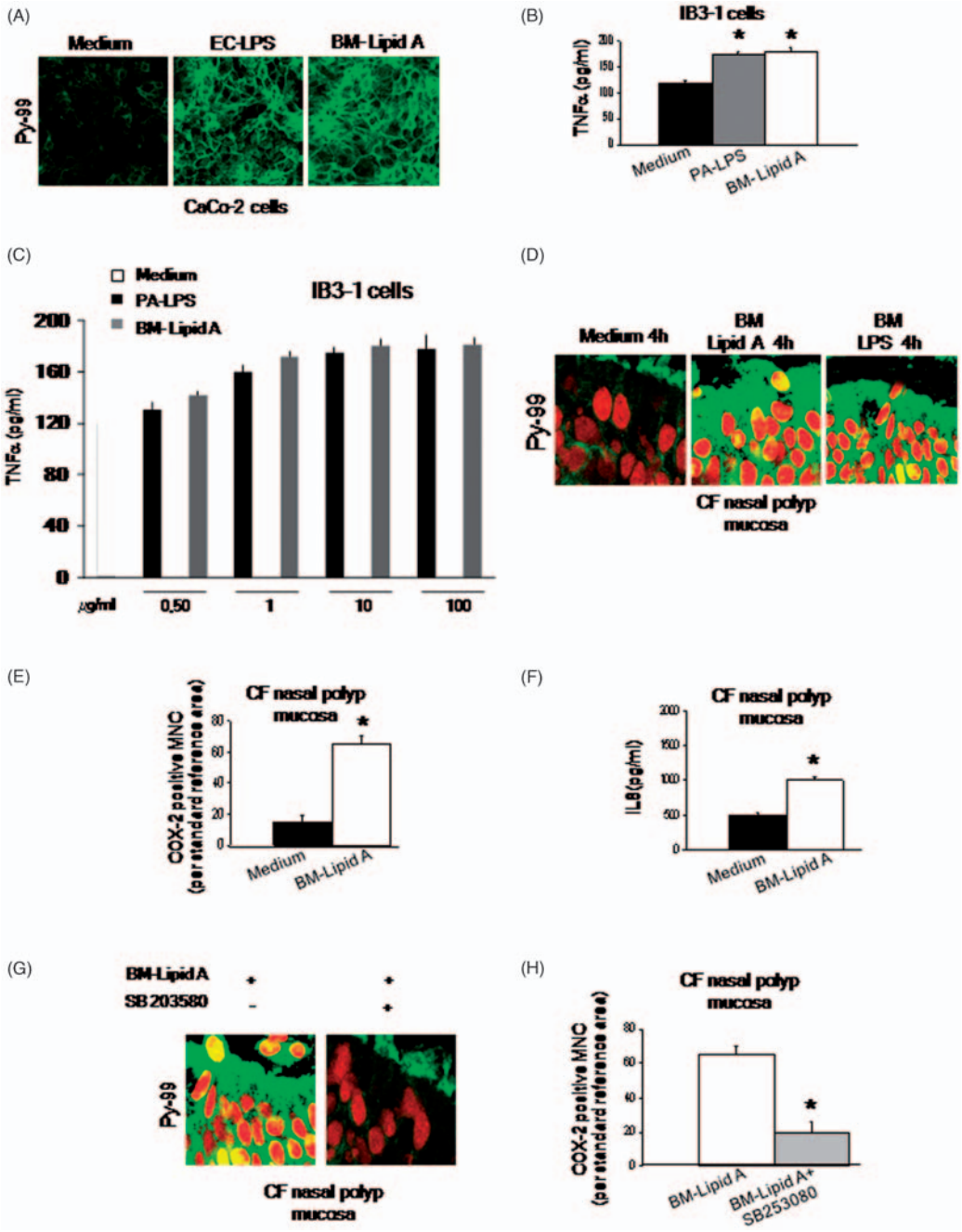


Fig. 5. (A) Confocal images of CACO-2 cells incubated with medium alone, *E. coli* LPS or *B. multivorans* lipid A and immunostained with Py99 (green). *Burkholderia multivorans* lipid A challenge for 24 h induced an impressive increase of epithelial phosphotyrosine expression (Py99, green) in CACO-2 cell lines. (B) TNF-α secretion in IB3-1 cell line (mean, SEM, $n = 3$, $^*P < 0.05$ versus medium). (C) TNF-α secretion in IB3-1 cell line upon incubation with 0.5, 1, 10, 100 µg/ml *P. aeruginosa* LPS or *B. multivorans* lipid A. (mean, SEM, $n = 3$, $P > 0.5$ between *P. aeruginosa* LPS or *B. multivorans* lipid A at all tested concentrations). (D) Confocal images of cystic fibrosis nasal mucosa incubated with medium alone, *B. multivorans* lipid A or *B. multivorans* LPS and immunostained with Py99 (green). *Burkholderia multivorans* lipid A and *B. multivorans* LPS challenge for 4 h induced an impressive increase of epithelial phosphotyrosine expression (Py99, green) in cystic fibrosis nasal mucosa. CyTRAK orange (red) nuclear counterstaining. (E) Induction of COX-2 protein expression by mucosal mononuclear cells (MNCs) following *B. multivorans* lipid A challenge (24 h). Mean (SD) number of COX-2 positive MNCs per mm^2 of mucosa after challenge with medium alone or *B. multivorans* lipid A ($^*P < 0.01$ versus samples cultured with medium alone). (F) IL-8 protein expression in culture supernatants after 4 h of *B. multivorans* lipid A challenge of nasal polyp explants from cystic fibrosis patients (mean, SEM, $n = 5$ $^*P < 0.05$ versus medium). (G) Confocal images of cystic fibrosis nasal mucosa incubated with *B. multivorans* lipid A or *B. multivorans* lipid A + SB253080 and immunostained with Py99 (green). Treatment with SB203580 totally prevented Py-99 up-regulation induced by *B. multivorans* lipid A challenge. (H) Inhibition of the p38-MAP-k pathway reduced induction of COX-2 protein expression by mucosal mononuclear cells induced by *B. multivorans* lipid A challenge. Mean (SD) number of COX-2 positive MNCs per mm^2 of mucosa after challenge with *B. multivorans* lipid A or *B. multivorans* lipid A added with SB203580 ($^*P < 0.05$ versus samples cultured with *B. multivorans* lipid A).

remarkably major mono-phosphorylated tetra-acylated lipid A species which may bear (or not) a further Ara4N residue (Fig. 4).

It is tempting to speculate that, within the same architectural framework, lipid A undergoes post-biosynthesis modifications and bioactivity modulation also depending on LPS size, *i.e*. the putative presence of the *O*-polysaccharide. This would explain, in case of *B. multivorans* LPS fraction, the existence of a *bis*-phosphorylated and penta-acylated lipid A as major species in the presence of a LOS,[24] while monophosphorylated and tetracylated species are present in case of a LPS. Therefore, the existence of a heterogeneous lipid A mixture that yields from a typical LPS preparation of several Gram-negative micro-organisms would, to a certain extent, have been explained by the different origin, *i.e*. LOS or LPS. Further studies are, however, needed to ascertain that acylation pattern of LPSs/LOSs of laboratory strains is identical to the *in vivo* acylation patterns.

The mechanisms responsible for controlling lipid A biosynthesis remain unclear, though recent reports have elucidated the pathways for fatty acids and aminoarabinose biosynthesis.[25] By analogy with *Enterobacteriaceae* lipid A biosynthesis, the presence of under-acylated and glycosylated (by Ara4N) lipid A species must be considered as a post-biosynthetic strategy following environmental pressure. The esterification of phosphate by Ara4N can be deemed as critical for bacterial survival. In fact, an important component of host response is the production of cationic peptides which act as antimicrobial molecules by linking to lipid A. An advantageous reply of the bacterium is a covalent modification of lipid A consisting in the addition of Ara4N, thus, reducing the net charge and ion attraction for the peptides.

The finding of such lipid A modifications in *B. multivorans* C1576 implies the presence of several enzymes that process it once its biosynthesis is accomplished, more likely at the level of Kdo_2–lipid A.[2,26] As a consequence, enzymes like the *E. coli* analogues of ArnT catalyzing the transfer of Ara4N and PagL for the primary fatty acid hydrolysis and *Francisella* LpxE analogue for the anomeric phosphate hydrolysis might be found and identified in *B. multivorans* C1576.[26]

Within this frame, it was interesting to detect, for the first time in *Burkholderia*, a particularly underacylated form, the lipid IVa analogue species **5**, which obviously derives from the complete penta-acyl lipid A by a successive selective enzymatic hydrolysis of the secondary fatty acid and anomeric phosphate (and Ara4N). This particular species is clearly reminiscent in structure of the lipid IVa endotoxin antagonist for the trimolecular LPS receptor complex TLR4–MD2–CD14; it would be important to ascertain if it gives any particular contribution to the overall bioactivity of the lipid A fraction. Work is in progress for its chemical synthesis.

Further elucidation of controllers of glycosylation, phosphorylation and acylation status may offer the development of therapeutic strategies and new treatments for the management of *Burkholderia* infections in dystic fibrosis.

In this work, it has also been demonstrated that lipid A is effective in triggering an inflammatory response in cystic fibrosis airways. By a multifaceted approach using either bronchial epithelial cell lines or human airways mucosal biopsies, it has been shown that the lipid A from *B. multivorans* is as effective as the LPS from *P. aeruginosa* in inducing early features of innate immunity activation in cystic fibrosis biopsies. The culture model used represents a good and interesting approximation to *in vivo* studies since all the anatomical connections are retained and all cell types (epithelial, myeloid, lymphoid) still interact with neighboring cells within their natural environment. Nasal polyps may complicate cystic fibrosis and need surgical excision. Moreover, it has been demonstrated that nasal mucosa provides a suitable representation of cystic fibrosis chronic airways inflammation.[18] We have already used *ex vivo* cultures of explants of nasal polyps to investigate the airway inflammatory response to environmental triggers.[18] In such a model, we demonstrated that cystic fibrosis nasal polyp mucosa is highly responsive to *P. aeruginosa* LPS that induces a cascade of events starting with activation of epithelial cells, cytokine production and neutrophil recruitment to the upper mucosal compartment. In particular, we demonstrated that *P. aeruginosa* LPS stimulation induces early epithelial tyrosine phosphorylation, p38-MAPK phosphorylation, and the potent neutrophil chemo-attractant and activator IL-8, that recruits large numbers of neutrophils into the airways. We have also demonstrated that the inhibition of the p38-MAPK pathway is effective in controlling *P. aeruginosa* LPS induced inflammatory response.

CONCLUSIONS

Lipid A is a potent trigger of inflammatory response and induces IL-8 secretion and epithelial activation by triggering the p38-MAPK pathway. The inhibition of p38-MAPK pathway is effective in controlling the features of inflammation induced upon *B. multivorans* lipid A stimulation. These inflammatory features are similar to those induced upon *P. aeruginosa* LPS challenge both in an epithelial cell line and in nasal polyp mucosa.

Together, these results demonstrate that lipid A of *B. multivorans* is endowed with pro-inflammatory

activity and also provide evidence that lipid A is at least one of the factors responsible for the pathogenicity of the *B. multivorans* in patients with cystic fibrosis.

ACKNOWLEDGEMENTS

The authors are grateful to Prof. J.R.W. Govan for the kind gift of the strain *B. multivorans* C1576. ESI mass spectra were run at the Centro Servizi Polivalenti di Ateneo (University of Trieste). This study was supported by the Italian Cystic Fibrosis Research Foundation (grant FFC#11/2006) and by the Italian 'Ministero dell'Istruzione, dell'Università e della Ricerca', (PRIN 2007).

REFERENCES

1. Pier GB. *Pseudomonas aeruginosa* lipopolysaccharide: a major virulence factor, initiator of inflammation and target for effective immunity. *Int J Med Microbiol* 2007; **297**: 277–295.
2. Raetz CRH, Whitfield C. Lipopolysaccharide endotoxins. *Annu Rev Biochem* 2002; **71**: 635–700.
3. Munford RS. Sensing Gram-negative bacterial lipopolysaccharides: a human disease determinant?. *Infect Immun* 2008; **76**: 454–465.
4. Silipo A, De Castro C, Lanzetta R, Parrilli M, Molinaro A. Lipopolysaccharides. In: König H, Claus H, Varma A., (eds) *Prokaryotic Cell Wall Compounds. Structure and Biochemistry*. Heidelberg: Springer, 2010 (forthcoming).
5. Zähringer U, Lindner B, Rietschel ETh. Molecular structure of lipid A, the endotoxic center of bacterial lipopolysaccharides. *Adv Carbohydr Chem Biochem* 1994; **50**: 211–276.
6. Akira S, Uematsu S, Osamu T. Pathogen recognition and innate immunity. *Cell* 2006; **124**: 783–801.
7. Beutler B, Rietschel ETh. Innate immune sensing and its roots: the story of endotoxin. *Nat Rev Immunol* 2003; **3**: 169–176.
8. Medzhitov R. Toll-like receptors and innate immunity. *Nat Rev Immunol* 2001; **1**: 135–145.
9. Seydel U, Oikawa M, Fukase K, Kusumoto S, Brandenburg K. Intrinsic conformation of lipid A is responsible for agonistic and antagonistic activity. *Eur J Biochem* 2000; **267**: 3032–3039.
10. Govan JR, Brown AR, Jones AM. Evolving epidemiology of *Pseudomonas aeruginosa* and the *Burkholderia cepacia* complex in cystic fibrosis lung infection. *Future Microbiol* 2007; **2**: 153–164.
11. Whiteford ML, Wilkinson JD, McColl JH *et al*. Outcome of *Burkholderia* (*Pseudomonas*) *cepacia* colonisation in children with cystic fibrosis following a hospital outbreak. *Thorax* 1995; **50**: 1194–1198.
12. Mahenthiralingam E, Coenye T, Chung JW *et al*. Diagnostically and experimentally useful panel of strains from the *Burkholderia cepacia* complex. *J Clin Microbiol* 2000; **38**: 910–913.
13. Westphal O, Jann K. Bacterial lipopolysaccharides: extraction with phenol-water and further applications of the procedure. *Methods Carbohydr Chem* 1995; **5**: 83–91.
14. Silipo A, Molinaro A, Cescutti P *et al*. Complete structural characterization of the lipid A fraction of a clinical strain of *Burkholderia cepacia* genomovar I lipopolysaccharide. *Glycobiology* 2005; **15**: 561–570.
15. Silipo A, Lanzetta R, Amoresano A, Parrilli M, Molinaro A. Ammonium hydroxide hydrolysis: a valuable support in the MALDI-TOF mass spectrometry analysis of lipid A fatty acid distribution. *J Lipid Res* 2002; **43**: 2188–2195.
16. Leontein K, Lönngren J. Determination of the absolute configuration of sugars by Gas-Liquid Chromatography of their acetylated 2-octyl glycosides. *Methods Carbohydr Chem* 1978; **62**: 359–362.
17. Ciucanu I, Kerek F. A simple method for the permethylation of carbohydrates. *Carbohydr Res* 1984; **131**: 209–217.
18. Raia V, Maiuri L, Ciacci C *et al*. Inhibition of p38 mitogen activated protein kinase controls airway inflammation in cystic fibrosis. *Thorax* 2005; **60**: 773–780.
19. Maiuri L, Lucani A, Giardino I *et al*. Tissue transglutaminase activation modulates inflammation in cystic fibrosis via PPARgamma down-regulation. *J Immunol* 2008; **180**: 7697–7705.
20. De Soyza A, Ellis CD, Khan ACM, Corris PA, Demarco de Hormaeche R. *Burkholderia cenocepacia* lipopolysaccharide, lipid A, and proinflammatory activity. *Am J Respir Crit Care Med* 2004; **170**: 70–77.
21. De Soyza A, Silipo A, Lanzetta R, Govan JR, Molinaro A. Chemical and biological features of *Burkholderia cepacia* complex lipopolysaccharides. *Innate Immun* 2008; **14**: 127–144.
22. Sforza S, Silipo A, Molinaro A, Marchelli R, Parrilli M, Lanzetta R. Determination of fatty acid positions in native lipid A by positive and negative electrospray ionization mass spectrometry. *J Mass Spectrom* 2004; **39**: 378–383.
23. Molinaro A, Lindner B, De Castro C *et al*. The structure of the lipid A of the lipopolysaccharide from *Burkholderia caryophylli* possessing a 4-amino-4-deoxy-L-arabinopyranose-1-phosphate residue exclusively in glycosidic linkage. *Chem Eur J* 2003; **9**: 1542–1548.
24. Ieranò T, Silipo A, Sturiale L *et al*. The structure and proinflammatory activity of the lipopolysaccharide from Burkholderia multivorans and the differences between clonal strains colonizing pre and posttransplanted lungs. *Glycobiology* 2008; **18**: 871–881.
25. Ortega XP, Cardona ST, Brown AR *et al*. A putative gene cluster for aminoarabinose biosynthesis is essential for *Burkholderia cenocepacia* viability. *J Bacteriol* 2007; **189**: 3639–3644.
26. Raetz CRH, Reynolds CM, Trent MS, Bishop RE. Lipid A modification systems in Gram-negative bacteria. *Annu Rev Biochem* 2007; **76**: 295–329.